Density, viscosity and excess properties of aqueous solution of 2-(2-Diethylaminoethoxy)ethanol (DEAE-EO)

Alain Valtz, Frédérick de Meyer, Christophe Coquelet

Density, viscosity and excess properties of aqueous solution of 2-(2-Diethylaminoethoxy)ethanol (DEAE-EO)

Alain Valtz[1], Frédérick de Meyer[2,1], Christophe Coquelet[3,1,*]

1 Mines Paris PSL University, CTP-Centre of Thermodynamics of Processes, 35 Rue Saint Honoré, 77305 Fontainebleau, France.

2 TotalEnergies S.E., OneTech, Gas and Low Carbon, CO_2 and Sustainability R&D, 2 Place Jean Millier, 92078 Paris, France.

3 Université de Toulouse, IMT Mines Albi, CNRS UMR 5302, Centre Rapsodee Campus Jarlard, 81013 Albi CT Cedex 9, France.

Keywords: Aqueous solvent, alkanolamine, CO_2 capture, gas processing, data treatment

Abstract – A complete study of thermophysical properties concerning the 2-(2-diethylaminoethoxy)ethanol (DEAE-EO) + water binary system is realized. Density, speed of sound, dynamic and kinematic viscosities and refractive index measurements have been performed at atmospheric pressure, using a vibrating tube densitometer, a falling ball viscosimeter, and a refractometer for pure DEAE-EO, pure water, and for aqueous solutions of DEAE-EO, from 278.15 to 323.15 K. The thermal expansion was calculated from density data. Excess Gibbs energy of flow and the corresponding excess entropy of flow were also calculated considering dynamic viscosity and density data. Excess molar properties (volume, isobaric expansion coefficient, Gibbs energy of flow and square of refractive index) were calculated and the Redlich-Kister equations were applied to correlate the data. Thermophysical properties of aqueous DEAE-EO (50 mol%) and Methyldiethanolamine (MDEA) (50 mol%) solutions were compared for their application in absorption of acid gases.

*: Corresponding author, Email: Christophe.coquelet@mines-albi.fr

1. Introduction

In this paper, we have studied the densities, speed of sound, viscosities and refractive index of mixtures composed of water and one potential co-solvent, 2-(2-Diethylaminoethoxy)ethanol (DEAE-EO), also known as Diethylaminoethoxyethanol (DEAEE) ($C_8H_{19}NO_2$ CAS number 140-82-9). DEAE-EO is a tertiary amine, of interest because of its structural characteristic, the ether group. DEAE-EO has mainly been studied in the context of acid gas treatment (CO_2 and (selective) H_2S removal) and anthropogenic CO_2 capture [1-6] or as a catalyst to produce polyurethane foams [7]. Pure DEAE-EO is liquid at standard conditions, soluble in water, it has a boiling point of 374 K at a pressure of 1.3 kPa, a flash point at 369 K, a specific gravity of 0.94 and a refractive index of 1.45 [8].

DEAE-EO is structurally close to Diethylaminoethanol (DEAE). DEAE is fully miscible with water, has a boiling point of 436 K at 101.33 kPa, a flash point around 323 K, a specific gravity of 0.89, a refractive index of 1.44 at 293.15 K and a pKa of 9.87 at 293.15 K according to pubchem website [9]

Chowdhury et al. [1], [2] studied DEAE-EO as part of a large screening study of tertiary amines for CO_2 absorption and found that, compared to MethylDiEthanolAmine (MDEA), at constant amine weight concentration, DEAE-EO shows a more than two times higher CO_2 absorption rate, a higher CO_2 absorption capacity (Vapor-Liquid Equilibrium measurements), a higher cyclic CO_2 absorption capacity and a similar CO_2 absorption heat. The CO_2 absorption properties of DEAE were found to be slightly better than DEAE-EO, despite the higher pKa value of DEAE-EO compared to DEAE. Compared to all tertiary amines tested, the CO_2 absorption properties of DEAE-EO are moderate. Orlov et al. [6] found a CO_2 absorption rate in aqueous DEAE-EO comparable to MDEA, at constant molar amine concentration.

As part of large screening study of solvents for CO_2 capture Hartono et al. [3] studied DEAE-EO to understand the impact of the ether group. They measured the pKa value of 10.15 for DEAE-EO at 298.15 K. It is thus significantly more basic than MDEA (pKa = 8.6). The CO_2 absorption rate and cyclic capacity were found to be rather high, which is in accordance with the relatively high pKa value. The loaded (μ=5.03 mPa.s) and lean (μ=4.21 mPa.s) solvent viscosity were also measured and found to be very similar to other tertiary amines.

Shoukat et al. [4] screened water-lean tertiary amine solvents for H_2S absorption and found a higher loading for DEAE-EO – Ethylene Glycol compared to aqueous MDEA at the same amine weight concentration. Orlov et al. [5] report that the CO_2 absorption in pure DEAE-EO is 5 times lower (mole fraction solubility of 0.02) compared to pure MDEA at atmospheric pressure.

Due to Hydrogen bonding, the ether group of DEAE-EO is expected to modify the intermolecular interactions with water. This should be reflected in the excess properties, which are very useful to understand the mixing state in terms of intermolecular interactions. Information concerning molecular interactions is required for the design of solvents for industrial applications.

First, new experimental measurements of density and excess volume for the binary mixture composed of water and DEAE-EO are presented. Then, these new experimental excess volumes are correlated by the Redlich-Kister equation [10]. Also, the same type of correlation will be used to correlate excess dynamic viscosity and refractive index data. To the knowledge of the authors, there is no data concerning the thermophysical properties of pure DEAE-EO and mixtures with water in the open literature. Finally, thermophysical properties of aqueous MDEA (13 mol%) and aqueous DEAE-EO (13 mol%) are compared in the context of utilization of aqueous DEAE-EO solvent for acid gas absorption.

2. Experimental details

2.1. Materials purities and suppliers

The chemical species, suppliers, purity, and refractive index are presented in Table 1. The different mixture compositions are prepared gravimetrically. Water was purified by a Millipore Direct-Q5UV system with a 0.22 µm membrane.

Table 1: Chemical sample

Compound	*CAS Number*	*Formula*	*Supplier*	*Purity (GC[a])*	*Refractive index* (293.15 K)*	*nD*
Water	7732-18-5	H_2O	-	-	1.33299	1.3325[b]
2-(2-(diethylamino)ethoxy) ethanol (DEAE-EO)	140-82-9	$C_8H_{19}NO_2$	Fisher Scientific (TCI)	>98%	1.44878	1.45[c]
Methyl Diethanol Amine (MDEA)	105-59-9	$C_5H_{13}NO_2$	Aldrich	>99%	1.46954	1.469[c]

*: Apparatus; Anton Paar ABBEMAT 300 (λ=589nm), supplier accuracy +/- 0.0001, u(n)=6 $\times 10^{-5}$, (a) GC: Gas Chromatograph, (b): Value from Simulis Thermodynamics (Prosim, France), (c): Refractive index value given by the supplier.

2.2. Experimental method

-Density

The DSA5000M Anton Paar digital vibrating tube densimeter is used to measure the densities of the amine solutions. The oscillating period or frequency, measured by the densitometer, depends on the tube mass and therefore on the fluid density. Eq. 1 is used for relating the period of vibration, τ, to density, ρ:

$$\rho = a + b\,\tau^2 \quad (1)$$

where a and b are constants to be adjusted. For these purposes we have used bi-distilled and degassed water, and dry air, at 293.15 K. Supplier accuracy (a) on measured density is estimated lower than 0.01 kg.m^{-3}. The calibration is realised following recommended procedure form supplier: ultra-pure water and dry air are the two reference fluids. During measurement, if the measured value is constant during300 seconds ($\pm 5\times10^{6}$ g.cm^{3}), the experimental data is validated. Chirico et al. [11] recommend to include the purity of the chemical species to estimate the relative density uncertainty (Eq. 2).

$$u_r(\rho) = \xi(1 - x_s) \quad (2)$$

with ξ the presumed difference in density between the compound and the impurity (the authors recommend ξ=0.1) and x_s the purity. Details on the global uncertainty calculation are given by Eq. 3. One platinum resistance thermometer with 0.01 K accuracy is used for temperature measurements. The sample densities are then measured at thermal equilibrium for various temperatures. The speed of sound with an accuracy of 0.5 m.s^{-1} can also be measured by our densitometer (see supporting information for more details).

$$u = \sqrt{\left(\frac{a}{\sqrt{3}}\right)^2 + \left(\rho \times u_r(\rho)\right)^2} \quad (3)$$

-Viscosity

An Anton Paar LOVIS 2000 ME viscometer is used to measure the viscosity of the aqueous solutions. Our viscosimeter is a modular instrument to be coupled with the densimeter DSA5000M. The solution sample is filled into a glass capillary (diameter of 1.59 mm) which is introduced into a temperature-controlled capillary block. This block can be inclined at a variable predefined angle according to the calibration performed. The capillary had already been calibrated with appropriate standard fluids (see Reference Manual of Lovis [12]). Calibration is realized considering standard oils with values memorized by the equipment. If relative deviations are lower than 0.1%, the equipment is considered as calibrated, if not, a new calibration procedure is realized until the relative deviation is lower than 0.1%. 6 cycles of measurements are considered for the repeatability. The experimental method of LOVIS 2000 ME viscometer is based on the falling ball method. The falling time of a steel ball in the capillary tube filled with the sample fluid is measured. The falling time is also measured considering different angles of inclination of the tube. It automatically provides the viscosity value for the temperature studied. The equation governing this principle (i.e. the calibration curve of the instrument) is given by Eq. 4.

$$\eta = K_1 * (\rho_K - \rho_S) * t_1 \quad (4)$$

where η is the dynamic viscosity of the sample solution in mPa.s; K_1 is the calibration constant of the measuring system; ρ_K is the ball (steel) density in g.cm^{-3}; ρ_S is the sample density in g.cm^{-3}, measured by the instrument, and t_1 is the rolling time in seconds. The estimate of viscosity uncertainty depends on the uncertainty of density. The calculation of the uncertainty is given by Eq. 5.

$$u = \sqrt{\left(\frac{u_B}{\sqrt{3}}\right)^2 + \left(\frac{s}{\sqrt{N}}\right)^2} \quad (5)$$

u_B , linked to the accuracy of the instrument, is equal to the 0.5% of the measured value for the LOVIS viscometer (given by Manual of Lovis |12]). The second term is the standard deviation (s) of the average of three different measurement cycles (we have considered 3 cycles). When just one cycle of measurements is performed, the uncertainty of the experimental data corresponds to the uncertainty of the instrument used (u_{RB}). More information concerning uncertainty estimation is given in the Supporting Information of Cremona et al. [13]. Also, following the recommendation of Huber et al. [14], we have considered a relative expanded uncertainty equal to $U_r(\eta)=0.01$.

The refractometer from Anton Paar ABBEMAT 300 with an accuracy of measurement equal to +/- 0.0001 is used to measure the refractive index of the DEAE-EO aqueous solutions. The refractive index was measured at 293.15 K. Atmospheric pressure is measured by a GE Druck DPI 142 Barometric Indicator with an uncertainty $u_p = 0.029$ kPa. Considering the natural variation of

"atmospheric pressure" we can estimate the uncertainty of pressure measurement equal to $u_p = 0.3$ kPa.

- Preparation of mixture

An empty 20 cm^3 glass bottle is air-tight closed with a septum. The bottle is put under vacuum using a vacuum pump wherein a needle is introduced through the septum. To prepare the mixtures, the empty bottle is weighed, and then the less volatile component, freshly degassed, is introduced by means of a syringe. After weighing the bottle loaded with the first component, the more volatile one is added similarly and then the bottle is weighed again. The composition is calculated considering the difference between the different weighing and the respective molar mass of the chemicals. All weightings are performed using an analytical balance with 10^{-4} g accuracy and hence the uncertainty is estimated to be lower than $2x10^{-5}$ for mole fractions.

3. Results and Discussions

3.1. Pure component properties

The density values of pure chemical measured using the DSA 5000M Anton Paar densitometer are presented as a function of temperature in Table 2. Our data concerning DEAE-EO are new as no data was found in the open literature. Comparisons with literature data concerning pure water are presented in the Supporting Information and a good agreement is observed. The isobaric expansion coefficient ($\alpha_p = \frac{1}{v}\left(\frac{\partial v}{\partial T}\right)_p$) is calculated using density data. The molar volume data were correlated by a second order polynomial expression in the temperature range 283.15-343.15 K ($v = aT^2 + bT + c$ where a, b and c are the parameters adjusted on experimental data). The parameters are presented in Table S3 in Supporting Information. The derivative with respect to temperature of molar volume correlation is considered for the calculation of the thermal expansion data. Calculated values of the isobaric expansion coefficient and the dynamic viscosity data obtained with the LOVIS 2000 ME for DEAE-EO and water are presented in Table 2.

Table 2: Density[*], isobaric expansion coefficient[**] and dynamic viscosity[*] of pure components DEAE-EO and water studied at atmospheric pressure (p=101.33 kPa)[a]

	DEAE-EO			Water		
T / K	ρ / kg.m^{-3}	$\alpha_p \times 10^4 / K^{-1}$	η / mPa.s	ρ / kg.m^{-3}	$\alpha_p \times 10^4 / K^{-1}$	η / mPa.s
283.15	948	8.73	13.984	1000	1.34	1.306
288.15	944	8.79	11.203	999	1.75	1.138
293.15	940	8.86	9.131	998	2.15	1.002
298.15	935	8.93	7.546	997	2.56	0.890
303.15	931	8.99	6.318	996	2.96	0.797
308.15	927	9.05	5.349	994	3.36	0.719
313.15	923	9.12	4.575	992	3.76	0.653
318.15	919	9.18	3.949	990	4.15	0.596
323.15	914	9.24	3.436	988	4.55	0.547
328.15	910	9.30	3.013	986	4.94	0.504
333.15	906	9.35	2.661	983	5.33	0.466
338.15	902	9.41	2.365	981	5.71	0.433
343.15	897	9.47	2.113	978	6.09	0.404

[a]Expanded uncertainties (k=2) U(p)=0.3 kPa, U(T)=0.01 K, U(ρ)=1.0 kg.m^{-3} U(α_p)=2.2 10^{-5}K^{-1}, U$_r$(η)=0.01.

[*]: measured, [**]: calculated

3.2. Excess properties

Excess molar volumes

The measured density of aqueous DEAE-EO solutions over the entire range of mole fractions x_1 and temperature range between (283.15 and 343.15) K are listed in Table 2. Density data were used to calculate the excess volume. The excess molar volumes v^E, are calculated using Eq. 6.

$$v^E = v - x_1 v_1^0 - x_2 v_2^0 \quad (6)$$

where x_1 and x_2 represent mole fractions and v_1^0 and v_2^0 are the molar volumes of components 1 and 2, respectively. v stands for the molar volume of mixture. Using the measured density ρ, Eq. 5 can be rewritten as:

$$v^E = \left[\frac{x_1 M_1 + x_2 M_2}{\rho}\right] - \frac{x_1 M_1}{\rho_1^0} - \frac{x_2 M_2}{\rho_2^0} \quad (7)$$

where M_1 and M_2 are the molar masses, ρ_1^0 and ρ_2^0 the densities of components 1 and 2, respectively. ρ stands for the density of the mixture. Maximum uncertainty resulting in the calculation of v^E is estimated to be less than 0.0011 $cm^3.mol^{-1}$ using Eqs. 8-10.

$$u_{\rho m} = \sqrt{u_\rho^2 + u_x^2} \quad (8)$$

$$u_{x1} = x_1 x_2 u_m \sqrt{\frac{1}{(m_1)^2} + \frac{1}{(m_2)^2}} \quad (9)$$

$$u_{v^E} = \sqrt{\left(\left(\frac{x_1 M_1 + x_2 M_2}{\rho_m^2}\right)^2 + \left(\frac{x_1 M_1}{\rho_1^2}\right)^2 + \left(\frac{x_2 M_2}{\rho_2^2}\right)^2\right) u_{\rho m}^2 + \left(\frac{M_1 + M_2}{\rho_m} - \frac{M_1}{\rho_1} - \frac{M_2}{\rho_2}\right)^2 u_x^2} \quad (10)$$

With M_i the molar mass of component i, m_i the mass of component i, ρ_i the density of component i, ρ_m density of the mixture.

Isobaric expansion coefficients

As explained above, isobaric expansion coefficient data are calculated using density data measured for different composition and temperature and by considering a second order polynomial

expression for the molar volume for each composition (parameters are given in Table S3 in Supporting Information). Like excess molar volume, the excess molar thermal expansion α^E, is calculated using Eq. 11.

$$\alpha_p^E = \alpha - \phi_1 {\alpha_p}_1^0 - \phi_2 {\alpha_p}_2^0 \quad (11)$$

where $\phi_i = \frac{x_i v_i^0}{\sum_i x_i v_i^0}$ is the volume fraction of component i and ${\alpha_p}_1^0$ and ${\alpha_p}_2^0$ are the molar isobaric expansion coefficient of pure components 1 and 2, respectively. The analysis of excess isobaric expansion coefficients is very important as it considers the influence of temperature in the variation of molar volume.

The uncertainty in isobaric expansion coefficient is linked to the uncertainty in density, the accuracy of the derivative with respect to temperature, and the uncertainty in molar fraction. Eq. 12 gives the expression.

$$u_{\alpha m} = \sqrt{{u_{\alpha_p}}^2 + {u_x}^2} \quad (12)$$

The uncertainty in composition is given by Eq. 9. For the isobaric expansion coefficient, uncertainty is given by Eq. 13.

$$u_{\alpha_p} = \sqrt{\left(\frac{\partial \alpha_p}{\partial \rho}\right)^2 u_\rho^2 + \left(\frac{\partial \alpha_p}{\partial T}\right)^2 u_T^2} \quad (13)$$

The value of u_α is equal to 1×10^{-5} K^{-1}. The uncertainty in excess isobaric expansion coefficient is given by Eq. 14. The value obtained is also close to 1.5×10^{-5} K^{-1}.

$$u_{{\alpha_p}^E} = \sqrt{(1 + \phi_1^2 + \phi_2^2) u_{\alpha_p}^2 + \left(\left({\alpha_p}_1^0\right)^2 + \left({\alpha_p}_2^0\right)^2\right) u_\phi^2} \quad (14)$$

With $u_{\phi_1} = \phi_1 \phi_2 u_{x_1} \sqrt{\left(\frac{1}{x_1^2} + \frac{1}{x_2^2}\right)}$. The value of u_{ϕ_i} is equal to 0.002.

Viscosity

The study of the kinematic viscosity (υ) instead of the dynamic viscosity (η) is preferred. In effect, according to Eyring theory [15], kinematic viscosity can be correlated using an Arrhenius type law. An

energy of activation of the flow is considered. This energy of activation is required to activate the flow or to produce a hole of requisite size for the translation to occur. The kinematic viscosity is linked to the dynamic viscosity by Eq. 15.

$$\upsilon = \eta v = hN_A e^{\left(\frac{-\Delta G^*}{RT}\right)} \quad (15)$$

Where *h* is Planck's constant, N_A Avogadro's number, *v* mass volume, *T* the temperature and ΔG^* is the activation Gibbs free energy of flow. This energy of activation can be written as the sum of two contributions: the ideal solution ΔG^{*id} and the excess part ΔG^{*E}. According to Eyring, this energy is linked to excess Gibbs free energy of the mixture ΔG^E which considers the molecular interaction between the two chemical species $\Delta G^{*E} = \sigma \Delta G^E$. σ is the proportionality factor. The excess Gibbs free energy given by Eq. 16 is calculated from a thermodynamic model (fugacity coefficient of component i in the mixture, φ_i and fugacity of pure component i at the same conditions of *T* and *P*, φ_i^0).

$$G^E = RT \sum_{i=1}^{N} x_i \left(ln\left(\varphi_i\right) - ln\left(\varphi_i^0\right)\right) \quad (16)$$

Eq. 17 gives the viscosity of an ideal solution. For the real mixture, the excess Gibbs free energy of flow can be expressed by Eq. 18.

$$\upsilon^{id} = (\eta v)^{id} = hN_a e^{\left(\frac{-\Delta G^{*id}}{RT}\right)} = x_1 ln(\eta_1 v_1) + x_2 ln(\eta v_2) \quad (17)$$

$$\Delta G^{*E} = RT\left(ln(\eta v) - x_1 ln(\eta_1 v_1) - x_2 ln(\eta v_2)\right) \quad (18)$$

3.3. Excess molar volumes

Usually the Redlich-Kister (RK) correlation [10] is chosen to correlate excess molar properties of binary systems. This equation is applied for the excess thermophysical properties (Y^E). Eq. 19 presents the correlation considering mole fraction. For the refractive index, we have considered the volume fraction instead of the molar composition

$$Y^E = x_1 x_2 \sum_i A_i (x_1 - x_2)^i \quad (19)$$

The coefficients (A_i) need to be determined. The method of calculation of the standard deviation of each parameter is given in Supporting Information file. The variance σ, corresponding to each fit, is calculated using Eq. 20.

$$\sigma = \sqrt{\left[\sum \frac{\left(Y^E - Y^E_{cal}\right)^2}{N-P}\right]} \quad (20)$$

where *P* is the number of parameters (A_n) and *N* represents the number of experimental data. The main difficulty of the RK treatment is the selection of the number of parameters A_i. In order to do that, it is recommended to investigate apparent molar properties. In our case, we have considered $\frac{v^E}{x_1 x_2}$ as a function of molar composition x_1. The $\frac{v^E}{x_1 x_2}$ quantity gives us useful information concerning volumetric properties, particularly at low concentration. Desnoyers and Perron [16] considered that this term is directly related to the apparent molar volume ($v_{i,\varphi}$) and can thus be assimilated to a thermodynamic property. Eq. 21 shows that $\frac{v^E}{x_1 x_2}$ is directly linked to the apparent molar volume.

$$\frac{v^E}{x_1 x_2} = \frac{v_{2,\varphi} - v_2^0}{x_1} = \frac{v_{1,\varphi} - v_1^0}{x_2} \quad (21)$$

where $v_{i,\varphi}$ is the apparent molar volume. Desnoyers and Perron indicate that the change of the $\frac{v^E}{x_1 x_2}$ slope can be attributed to various factors: the first one, the size and shape of molecules, the second one, the intermolecular interaction energy differences at infinite or close to infinite dilution (in effect, at infinite dilution, $\frac{v^E}{x_1 x_2}$ decreases like the apparent molar volume) and the third one, the formation of chemical complexes containing unlike molecules. There are two contributions for the apparent molar volume of a molecule: the volume of the molecule and the free volume space. By analysis of the evolution of $\frac{v^E}{x_1 x_2}$ as a function of x_1 we have selected the number of RK parameters (6) for the investigation of all excess thermophysical properties.

The partial molar volume $\overline{v_i}$ ($cm^3.mol^{-1}$) of each component *i* has been calculated using Eq. 22, with *V*, the volume of the mixture (cm^3).

$$\overline{v_i} = \left(\frac{\partial V}{\partial n_i}\right)_{T,P,n_j} \quad (22)$$

Differentiating Eq. 22 with respect to n_i and combining the result with Eq. 19 leads to equations for the partial molar volumes of the different species (Eqs. 23 and 24).

$$\overline{v_1} = v^E + v_1^* - x_2\left(\frac{\partial v^E}{\partial x_2}\right)_{T,P} \quad (23)$$

$$\overline{v_2} = v^E + v_2^* - x_1\left(\frac{\partial v^E}{\partial x_1}\right)_{T,P} \quad (24)$$

Using the Redlich-Kister equation, we can obtain the expression of partial molar volumes (Eqs. 25 and 26) with respect to x_i.

$$\overline{v_1} = v_1^* + x_2^2 \sum A_n (1 - 2x_2)^n + 2x_2^2 (1 - x_2) \sum nA_n (1 - 2x_2)^{n-1} \quad (25)$$

$$\overline{v_2} = v_2^* + (1 - x_2)^2 \sum A_n (1 - 2x_2)^n - 2x_2 (1 - x_2)^2 \sum nA_n (1 - 2x_2)^{n-1} \quad (26)$$

At infinite dilution Eqs 25 and 26 give Eqs. 27 and 28.

$$\overline{v_1^\infty} = v_1^* + \sum A_n (-1)^n \quad (27)$$

$$\overline{v_2^\infty} = v_2^* + \sum A_n \quad (28)$$

Concerning the uncertainty of molar volume at infinite dilution, it is given by Eq. 29.

$$u\left(\overline{v_i^\infty}\right) = \sqrt{u\left(v_i^*\right)^2 + \sum u(A_n)^2} \quad (29)$$

Table 3 presents the values of mixture densities and excess volumes. The measured densities at 293.15, 308.15 and 313.15 K over the entire range of mole fractions x_1 are plotted in Figure 1. One can see that starting from x_1=0, the density increases with increasing DEAE-EO concentration, reaches a maximum value for composition lower than 0.1 mole fraction, and then decreases. The composition of the solution corresponding to the maximum density decreases with temperature.

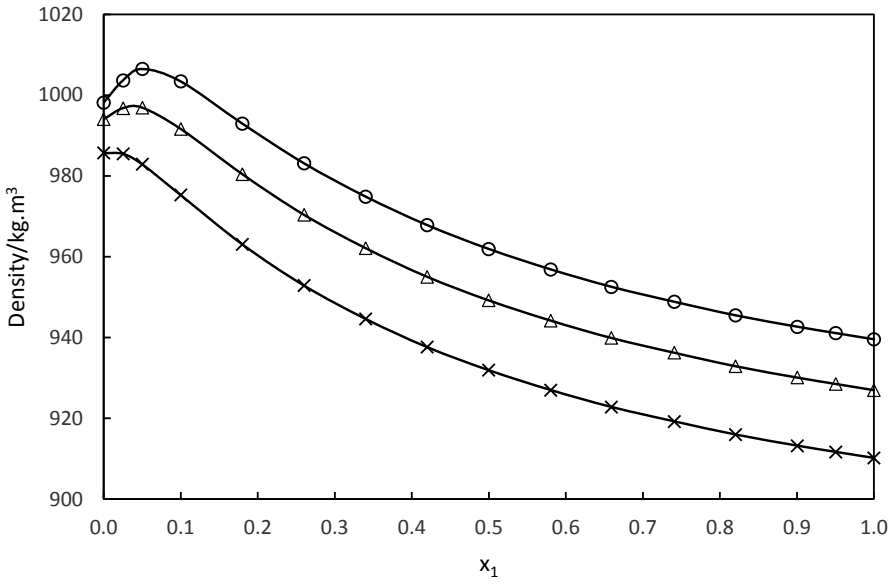

Figure 1: Density for DEAE-EO (1) + water (2) binary system as a function of DEAE-EO mole fraction at atmospheric pressure and 3 different temperatures: (○) 293.15 K, (Δ) 308.15 K, (×) 328.15 K.

Following Desnoyer's and Perron's recommendations on the utilization of the Redlich-Kister correlation for the data treatment, we have considered 6 Redlich-Kister parameters (presented in Table 4). Based on Redlich Kister formalism, $\frac{v^E}{x_1 x_2}$ is represented by a polynomial expression with each term expressed by $A_i(x_1 - x_2)^i$. If the shape of $\frac{v^E}{x_1 x_2}$ is not common, particularly at the extremity (close to each pure component), certainly, a polynomial expression with a high degree is required. For all the data treatment, we have considered 5 parameters. Figs. 2-3 present respectively, $\frac{v^E}{x_1 x_2}$ as a function of x_1 and v^E as a function of x_1, at 293.15 and 328.15 K. The excess molar volume is negative and we can observe that in absolute value, the excess volume is very important. This information supports the idea of a strong associative interaction between the two molecules. The objective of the following work is to better identify the interactions between the two molecules. The analysis of apparent molar volume does not reveal any original behavior. Hepler [17] in 1969 has observed that it was possible to identity the effect of solute in water as structure maker or structure breaker. He indicates the partial molar heat capacity is commonly negative in the case of

structured liquid and so $\left(\partial C_P/\partial P\right)_T$ should be negative. Eq. 30 presents the thermodynamic equation that relates heat capacity to the derivative of molar volume with respect to temperature.

$$\left(\frac{\partial C_P}{\partial P}\right)_T = -T\left(\frac{\partial^2 v}{\partial T^2}\right)_P \quad (30)$$

It is possible to evaluate the effect of the solute at infinite dilution on the structure of the liquid. The temperature dependence of the molar volume at infinite dilution and the second derivative is particularly meaningful because the sign of the second derivative $\left(\frac{\partial^2 v_1^\infty}{\partial T^2}\right)_P$ can be used as one criterion to justify if DEAE-EO is a structure breaker or structure maker. In Table 5 we present the values of molar volume of DEAE-EO and water at infinite dilution as a function of temperature calculated using Redlich-Kister parameters and Eqs. 31 and 32. Considering DEAE-EO, we can correlate the molar volume at infinite dilution using a second order polynomial expression (Eq. 31).

$$v_1^\infty = 0.00005623T^2 + 0.17289T + 99.71 \quad (31)$$

Using Eq. 35, we can calculate the second derivative with temperature and observe that $\left(\frac{\partial^2 v_1^\infty}{\partial T^2}\right)_P > 0$. This led to negative $\left(\frac{\partial C_P}{\partial P}\right)_T$ and so we can assume that DEAE-EO is a structure maker. It is due to the H-bonds between DEAE-EO and water (negative excess volume). Also, one should observe a decrease of the apparent molar volume (especially at low temperature) due to the possible existence of a complex due to hydrogen bonds between atoms of oxygen and hydrogen of water and DEAE-EO. This complex certainly exists for compositions very close to x_1=0 and it is surrounded by molecules of water due to strong hydrophobic interactions. At the opposite, in the DEAE-EO rich region, the system under study behaves in a regular manner. The shape of the curve $\frac{v^E}{x_1 x_2}$ is similar to the one presented by Coquelet et al. [18] for the hexamethyleimine (HMI) and water binary system. HMI doesn't have any -OH groups and has less possibilities to engage in hydrogen bonds. In Figure 3 we have plotted $\frac{v^E}{x_1 x_2}$ at 293.15 K for the MDEA + water (data from Bernal Garcia et al. [19]) and DiEthylEthanolAmine (DEAE) +water (data from Ma et al. [20]) binary systems. As we can see, the shapes of the 3 curves are not similar: with MDEA we have a minimum for a molar composition close to 0.2 but not for DEAE (the structure is similar to DEAE-EO without the ethoxy group). As shown by Coquelet et al. [18] for the binary systems including water, the curve $\frac{v^E}{x_1 x_2}$ presents, in general, a minimum at infinite dilution or close to infinite dilution state is the sign of the existence of hydrophobic interaction. With MDEA we have two -OH groups and only one with DEAE-EO (and one

ethoxy group). The real excess standard partial molar volume of DEAE-EO cannot be obtained by extrapolation of our data through the Redlich–Kister equation with 6 parameters and more density data in the very dilute region are required to better understand if DEAE-EO is really a structure maker or breaker.

Table 3: Densities[*] (ρ /kg.m^{-3}), excess molar volumes[**] (v^E/ cm^3.mol^{-1}), molar expansion[**] (α_p / K^{-1}) and excess molar expansion[**] (α_p^E /K^{-1}) for DEAE-EO *(1)* + water *(2)* binary system as a function of DEAE-EO mole fraction at atmospheric pressure (p=101.33 kPa)[a]

x_1	ρ	$\alpha_p \times 10^4$	v^E	$\alpha_p^E \times 10^4$	ρ	$\alpha_p \times 10^4$	v^E	$\alpha_p^E \times 10^4$	ρ	$\alpha_p \times 10^4$	v^E	$\alpha_p^E \times 10^4$	ρ	$\alpha_p \times 10^4$	v^E	$\alpha_p^E \times 10^4$	ρ	$\alpha_p \times 10^4$	v^E	$\alpha_p^E \times 10^4$
	T=283.15 K				T=288.15 K				T=293.15 K				T=298.15 K				T=303.15 K			
0.0000	1000	1.34	-	-	999	1.75	-	-	998	2.15	-	-	997	2.56	-	-	996	2.96	-	-
0.0250	1007	3.48	-0.385	0.70	1006	3.79	-0.377	0.67	1004	4.11	-0.370	0.064	1002	4.42	-0.364	0.062	999	4.73	-0.358	0.059
0.0500	1012	5.70	-0.758	1.91	1010	5.90	-0.734	1.81	1007	6.10	-0.712	0.171	1003	6.29	-0.693	0.161	1000	6.49	-0.675	0.151
0.1000	1011	7.41	-1.245	2.29	1007	7.54	-1.210	2.18	1003	7.68	-1.177	0.208	1000	7.81	-1.148	0.198	996	7.95	-1.120	0.188
0.1799	1001	8.02	-1.651	1.70	997	8.16	-1.616	1.65	993	8.29	-1.584	0.161	989	8.42	-1.555	0.156	985	8.56	-1.527	0.151
0.2600	991	8.27	-1.834	1.25	987	8.40	-1.804	1.23	983	8.52	-1.775	0.121	979	8.64	-1.747	0.118	975	8.77	-1.721	0.116
0.3400	983	8.38	-1.883	0.91	979	8.50	-1.856	0.90	975	8.62	-1.832	0.090	971	8.74	-1.808	0.089	966	8.86	-1.788	0.088
0.4199	976	8.49	-1.822	0.70	972	8.60	-1.800	0.70	968	8.71	-1.779	0.070	964	8.81	-1.758	0.069	959	8.92	-1.736	0.069
0.4998	970	8.51	-1.691	0.49	966	8.62	-1.674	0.50	962	8.72	-1.656	0.050	958	8.82	-1.640	0.050	953	8.92	-1.623	0.050
0.5803	965	8.55	-1.504	0.34	961	8.64	-1.489	0.35	957	8.74	-1.477	0.036	953	8.84	-1.465	0.036	948	8.93	-1.451	0.037
0.6592	961	8.58	-1.269	0.24	957	8.67	-1.258	0.24	953	8.76	-1.249	0.025	948	8.85	-1.239	0.025	944	8.94	-1.229	0.026
0.7408	957	8.62	-1.017	0.15	953	8.70	-1.011	0.16	949	8.79	-1.003	0.016	945	8.87	-0.996	0.017	940	8.95	-0.989	0.017
0.8203	954	8.68	-0.713	0.09	950	8.73	-0.709	0.09	945	8.81	-0.704	0.010	941	8.88	-0.700	0.010	937	8.96	-0.696	0.011
0.9004	951	8.71	-0.409	0.04	947	8.75	-0.408	0.04	943	8.83	-0.406	0.004	938	8.90	-0.404	0.005	934	8.97	-0.401	0.005
0.9503	949	8.73	-0.215	0.02	945	8.78	-0.213	0.02	941	8.85	-0.212	0.002	937	8.91	-0.210	0.002	933	8.98	-0.209	0.003
1.0000	948	1.34	-	-	944	8.79	-	-	940	8.86	-	-	935	8.93	-	-	931	8.99	-	-

[a]Expanded uncertainties (k=2) U(p)=0.3 kPa, U(T)=0.01 K, U(ρ)=1.0 kg.m^{-3} , U(x)=0.002, U(v^E)=0.011 cm^3.mol^{-1}, U(α_p)=2.2 10^{-5}K^{-1} , U(α_p^E)=4 10^{-5}K^{-1}

[*]: measured, [**]: calculated

Table 3: Continued

x_1	ρ	$\alpha_p \times 10^4$	v^E	$\alpha_p^E \times 10^4$	ρ	$\alpha_p \times 10^4$	v^E	$\alpha_p^E \times 10^4$	ρ	$\alpha_p \times 10^4$	v^E	$\alpha_p^E \times 10^4$	ρ	$\alpha_p \times 10^4$	v^E	$\alpha_p^E \times 10^4$	ρ	$\alpha_p \times 10^4$	v^E	$\alpha_p^E \times 10^4$
		T=308.15 K				T=313.15 K				T=318.15 K				T=323.15 K				T=328.15 K		
0.0000	994	3.36	-	-	992	3.76	-	-	990	4.15	-	-	988	4.55	-	-	986	4.94	-	-
0.0250	997	5.04	-0.353	0.056	994	5.35	-0.348	0.053	991	5.65	-0.344	0.051	989	5.96	-0.339	0.048	986	6.26	-0.335	0.045
0.0500	997	6.68	-0.659	0.141	994	6.87	-0.645	0.132	990	7.06	-0.627	0.122	987	7.25	-0.618	0.112	983	7.44	-0.606	0.103
0.1000	992	8.08	-1.094	0.178	988	8.21	-1.070	0.168	984	8.33	-1.049	0.158	979	8.46	-1.027	0.148	975	8.58	-1.007	0.139
0.1799	980	8.68	-1.500	0.146	976	8.81	-1.474	0.142	972	8.94	-1.452	0.137	968	9.06	-1.424	0.132	963	9.18	-1.400	0.128
0.2600	970	8.89	-1.696	0.114	966	9.00	-1.671	0.111	962	9.12	-1.647	0.109	957	9.24	-1.623	0.107	953	9.35	-1.599	0.104
0.3400	962	8.97	-1.764	0.088	958	9.08	-1.740	0.087	953	9.20	-1.710	0.086	949	9.31	-1.695	0.085	945	9.42	-1.672	0.085
0.4199	955	9.02	-1.716	0.068	951	9.12	-1.696	0.068	946	9.22	-1.680	0.067	942	9.32	-1.655	0.067	938	9.42	-1.634	0.067
0.4998	949	9.02	-1.607	0.051	945	9.12	-1.590	0.051	941	9.22	-1.574	0.051	936	9.31	-1.556	0.052	932	9.41	-1.538	0.052
0.5803	944	9.03	-1.439	0.038	940	9.12	-1.424	0.038	936	9.21	-1.409	0.039	931	9.30	-1.396	0.039	927	9.39	-1.380	0.040
0.6592	940	9.03	-1.219	0.027	936	9.11	-1.209	0.027	931	9.20	-1.203	0.028	927	9.28	-1.187	0.028	923	9.36	-1.174	0.029
0.7408	936	9.03	-0.983	0.018	932	9.11	-0.975	0.018	928	9.19	-0.957	0.019	924	9.27	-0.960	0.019	919	9.34	-0.951	0.020
0.8203	933	9.04	-0.692	0.011	929	9.11	-0.686	0.011	924	9.18	-0.691	0.012	920	9.26	-0.677	0.012	916	9.33	-0.670	0.013
0.9004	930	9.04	-0.400	0.005	926	9.11	-0.397	0.006	922	9.18	-0.397	0.006	917	9.25	-0.392	0.006	913	9.31	-0.388	0.006
0.9503	929	9.05	-0.211	0.003	924	9.11	-0.209	0.003	920	9.18	-0.201	0.003	916	9.24	-0.205	0.003	912	9.30	-0.203	0.003
1.0000	927	9.05	-	-	923	9.12	-	-	919	9.18	-	-	914	9.24	-	-	910	9.30	-	-

[a]Expanded uncertainties (k=2) U(p)=0.3 kPa, U(T)=0.01 K, U(ρ)=1.0 kg.m^{-3} , U(x)=0.002, U(v^E)=0.011 cm^3.mol^{-1}, U(α_p)=2.2 10^{-5}K^{-1} , U(α_p^E)=4 10^{-5}K^{-1}

Table 3: Continued

x_1	ρ	$\alpha_p \times 10^4$	v^E	$\alpha_p^E \times 10^4$	ρ	$\alpha_p \times 10^4$	v^E	$\alpha_p^E \times 10^4$	ρ	$\alpha_p \times 10^4$	v^E	$\alpha^E \times 10^4$
		T=333.15 K				T=338.15 K				T=343.15 K		
0.0000	983	5.33	-	-	981	5.71	-	-	978	6.09	-	-
0.0250	982	6.55	-0.331	0.042	979	6.85	-0.331	0.039	976	7.14	-0.324	0.037
0.0500	979	7.62	-0.595	0.093	975	7.80	-0.595	0.084	972	7.98	-0.576	0.074
0.1000	971	8.71	-0.988	0.129	967	8.83	-0.988	0.119	962	8.94	-0.952	0.110
0.1799	959	9.30	-1.376	0.123	954	9.42	-1.376	0.119	950	9.53	-1.330	0.114
0.2600	948	9.46	-1.576	0.102	944	9.57	-1.576	0.100	939	9.68	-1.528	0.097
0.3400	940	9.52	-1.649	0.084	936	9.63	-1.649	0.083	931	9.73	-1.603	0.083
0.4199	933	9.51	-1.614	0.066	929	9.61	-1.614	0.066	924	9.70	-1.571	0.065
0.4998	928	9.50	-1.520	0.052	923	9.59	-1.520	0.052	919	9.68	-1.480	0.052
0.5803	923	9.48	-1.365	0.040	918	9.56	-1.365	0.041	914	9.65	-1.330	0.041
0.6592	918	9.44	-1.162	0.029	914	9.52	-1.162	0.030	910	9.60	-1.135	0.031
0.7408	915	9.42	-0.941	0.020	911	9.49	-0.941	0.021	906	9.56	-0.920	0.021
0.8203	912	9.40	-0.663	0.013	907	9.46	-0.663	0.013	903	9.53	-0.648	0.014
0.9004	909	9.38	-0.385	0.007	905	9.44	-0.385	0.007	900	9.50	-0.376	0.007
0.9503	907	9.37	-0.202	0.003	903	9.43	-0.202	0.004	899	9.48	-0.197	0.004
1.0000	906	9.35	-	-	902	9.41	-	-	897	9.47	-	-

[a]Expanded uncertainties (k=2) U(P)=0.3 kPa, U(T)=0.01 K, U(ρ)=1.0 kg.m^{-3}, U(x)=0.002, U(v^E)=0.011 cm^3.mol^{-1}, U(α_p)=2.2 10^{-5}K^{-1} , U(α_p^E)=4 10^{-5}K^{-1}

Table 4: Excess molar volumes: Redlich-Kister parameters and deviation for DEAE-EO + water binary system.

T/K	Redlich Kister parameters										Variance σ/ $cm^3.mol^{-1}$, eq.20
	A_0	u(A_0)	A_1	u(A_1)	A_2	u(A_2)	A_3	u(A_3)	A_4	u(A_4)	
283.15	-6.70155	0.00025	4.0411	0.0006	-3.121	0.0016	2.474	0.0009	-1.044	0.0019	0.018
288.15	-6.64441	0.00016	3.9023	0.0004	-2.826	0.0011	2.380	0.0006	-1.187	0.0012	0.015
293.15	-6.59215	0.00010	3.7870	0.0002	-2.527	0.0007	2.285	0.0004	-1.353	0.0008	0.012
298.15	-6.53734	0.00006	3.6530	0.0001	-2.300	0.0004	2.256	0.0002	-1.448	0.0005	0.009
303.15	-6.48537	0.00004	3.5500	0.0001	-2.043	0.0003	2.185	0.0002	-1.611	0.0003	0.008
308.15	-6.43236	0.00003	3.4505	0.0001	-1.802	0.0002	2.101	0.0001	-1.806	0.0002	0.007
313.15	-6.37388	0.00003	3.3423	0.0001	-1.598	0.0002	2.085	0.0001	-1.935	0.0003	0.007
318.15	-6.31223	0.00004	3.2320	0.0001	-1.445	0.0003	2.076	0.0002	-2.013	0.0003	0.007
323.15	-6.24983	0.00006	3.1396	0.0001	-1.293	0.0004	2.055	0.0002	-2.097	0.0005	0.008
328.15	-6.18559	0.00007	3.0472	0.0002	-1.120	0.0005	2.047	0.0003	-2.230	0.0006	0.010
333.15	-6.12087	0.00009	2.9658	0.0002	-0.958	0.0006	2.030	0.0003	-2.358	0.0007	0.011
338.15	-6.04787	0.00011	2.8739	0.0002	-0.832	0.0007	2.057	0.0004	-2.437	0.0008	0.012
343.15	-5.97804	0.00013	2.7914	0.0003	-0.674	0.0009	2.060	0.0005	-2.586	0.0011	0.014

Table 5: Molar volume at infinite dilution for DEAE-EO *(1)* + water *(2)* binary system.

T/ K	v_1^{∞}/ cm^3.mol^{-1}	u(v_1^{∞})/ / cm^3.mol^{-1}	v_2^{∞}/ cm^3.mol^{-1}	u(v_2^{∞})/ / cm^3.mol^{-1}
283.15	153.8	0.01	13.0	0.01
288.15	154.2	0.01	13.2	0.01
293.15	155.3	0.01	13.3	0.01
298.15	156.3	0.01	13.5	0.01
303.15	157.4	0.01	13.6	0.01
308.15	158.4	0.01	13.6	0.01
313.15	159.4	0.01	13.7	0.01
318.15	160.4	0.01	13.9	0.01
323.15	161.4	0.01	14.0	0.01
328.15	162.4	0.01	14.1	0.01
333.15	163.4	0.01	14.2	0.01
338.15	164.4	0.01	14.4	0.01
343.15	165.3	0.01	14.5	0.01

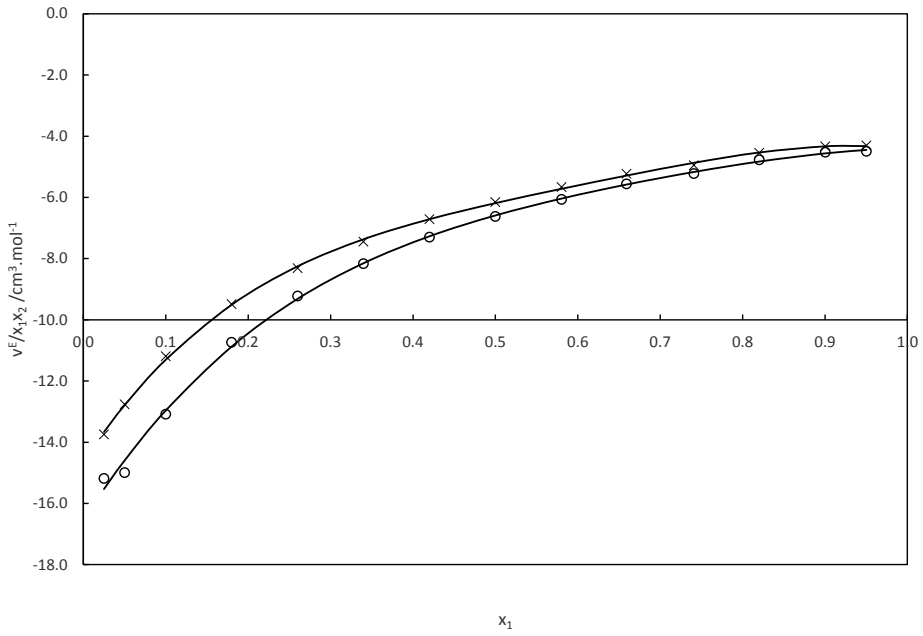

Figure 2: $\frac{v^E}{x_1 x_2}$ **for DEAE-EO (1) + water (2) system as a function of DEAE-EO mole fraction at atmospheric pressure and 2 different temperatures: (○) 293.15 K, (×) 328.15 K, solid line: Redlich-Kister correlation.**

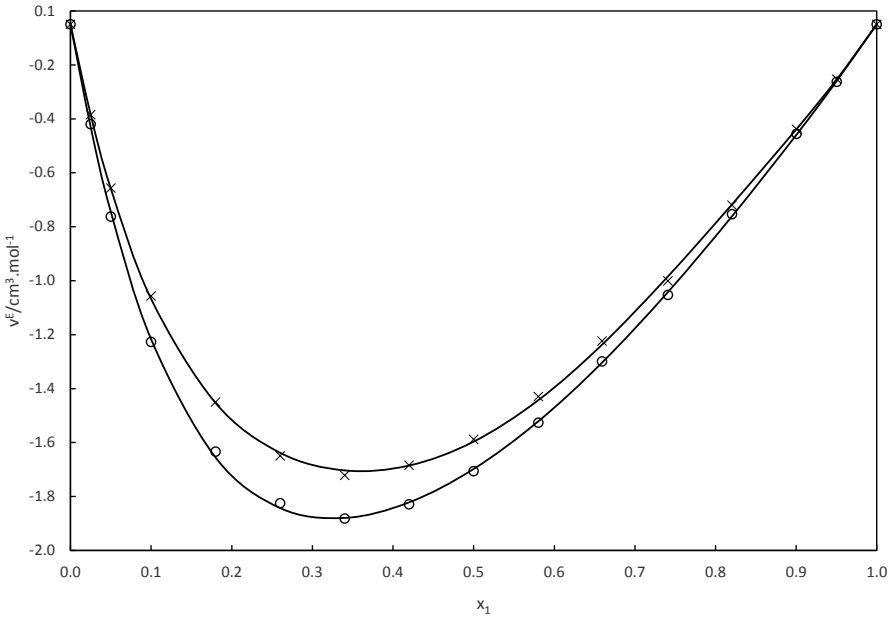

Figure 3: Excess molar volumes (v^E) for DEAE-EO (1) + water (2) binary system as a function of DEAE-EO composition at atmospheric pressure and 2 different temperatures: (○) 293.15 K, (×) 328.15 K, solid line: Redlich-Kister correlation.

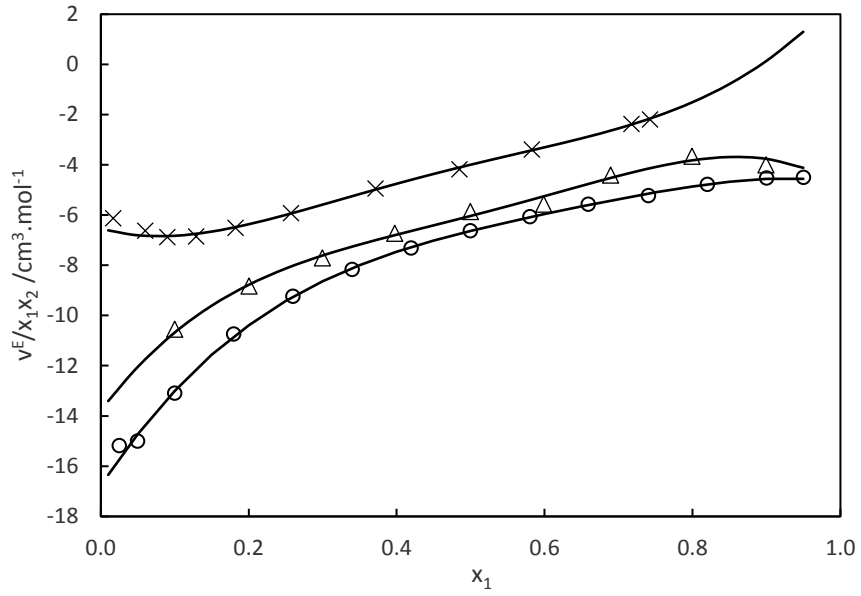

Figure 4: Comparison of $\frac{v^E}{x_1 x_2}$ for DEAE-EO + water (○), MDEA + water (×) (data from Bernal-Garcia et al. [21]) and DEAE + water (Δ) (data from Ma et al. [22]) binary systems as a function of amine mole fraction at atmospheric pressure and 293.15 K.

3.4. Isobaric expansion coefficients

The results concerning the isobaric expansion coefficients are presented in Table 3. We have also considered 5 parameters of the Redlich Kister equation for the data treatment. Table 6 presents the values of the Redlich-Kister parameters. According to Fig. 5, the excess isobaric expansion coefficient shows a maximum value for a DEAE-EO volumetric fraction close to 0.5. Regarding $\frac{{\alpha_p}^E}{\phi_1\phi_2}$ (see Fig. 6), we can observe that the maximum of the apparent isobaric expansion coefficient decreases as the temperature increases, and the DEAE-EO volumetric fraction corresponding to the maximum increases. This could be because the molecular interaction between the two chemicals, probably H-bonds between the two chemicals species, is strongly temperature-dependent and decreases in intensity with the temperature

Table 6: Isobaric expansion coefficients: Redlich-Kister parameters and deviation for DEAE-EO + water binary system.

T/K	Redlich Kister parameters										Variance $\sigma \times 10^4/K^{-1}$, eq.20
	$A_0 \times 10^4$	$u(A_0) \times 10^5$	$A_1 \times 10^4$	$u(A_1) \times 10^5$	$A_2 \times 10^4$	$u(A_2) \times 10^4$	$A_3 \times 10^3$	$u(A_3) \times 10^4$	$A_4 \times 10^4$	$u(A_4) \times 10^4$	
283.15	9.00	1.4	-2.737	5.1	-5.06	0.8	1.27	1.4	-10.74	1.5	0.025
288.15	8.61	1.3	-2.220	4.7	-4.75	0.7	1.16	1.3	-9.75	1.4	0.018
293.15	8.21	1.2	-1.712	4.2	-4.43	0.6	1.05	1.2	-8.77	1.2	0.016
298.15	7.82	1.0	-1.218	3.8	-4.10	0.6	0.94	1.1	-7.81	1.1	0.015
303.15	7.42	1.0	-0.726	3.5	-3.78	0.5	0.83	1.0	-6.83	1.0	0.013
308.15	7.03	0.9	-0.236	3.3	-3.49	0.5	0.72	0.9	-5.78	1.0	0.010
313.15	6.64	0.8	0.234	3.0	-3.16	0.4	0.62	0.9	-4.82	0.9	0.009
318.15	6.25	0.8	0.699	2.8	-2.83	0.4	0.51	0.8	-3.86	0.8	0.007
323.15	5.86	0.8	1.156	2.8	-2.50	0.4	0.40	0.8	-2.90	0.8	0.005
328.15	5.47	0.8	1.607	2.9	-2.17	0.4	0.29	0.8	-1.94	0.9	0.004
333.15	5.09	0.8	2.051	3.1	-1.85	0.5	0.19	0.9	-0.99	0.9	0.004
338.15	4.70	0.9	2.483	3.3	-1.50	0.5	0.09	1.0	-0.08	1.0	0.005
343.15	4.34	1.0	2.892	3.7	-1.19	0.5	-0.02	1.1	0.87	1.1	0.007

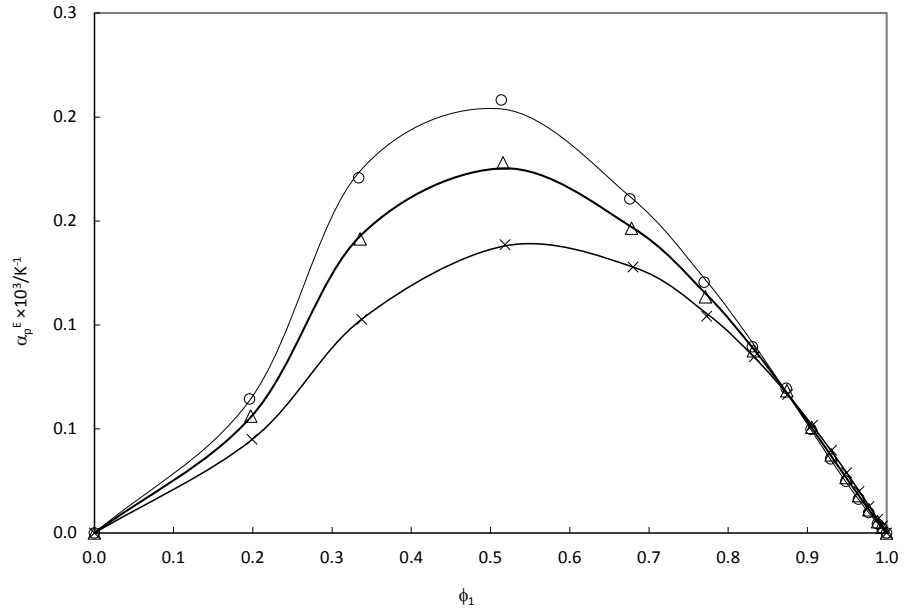

Figure 5: Excess molar isobaric expansion coefficient (α_p^E) for DEAE-EO (1) + water (2) binary system as a function of DEAE-EO composition at atmospheric pressure and 3 different temperatures: (○) 293.15 K, (Δ) 308.15 K, (×) 328.15 K, solid line: Redlich-Kister correlation.

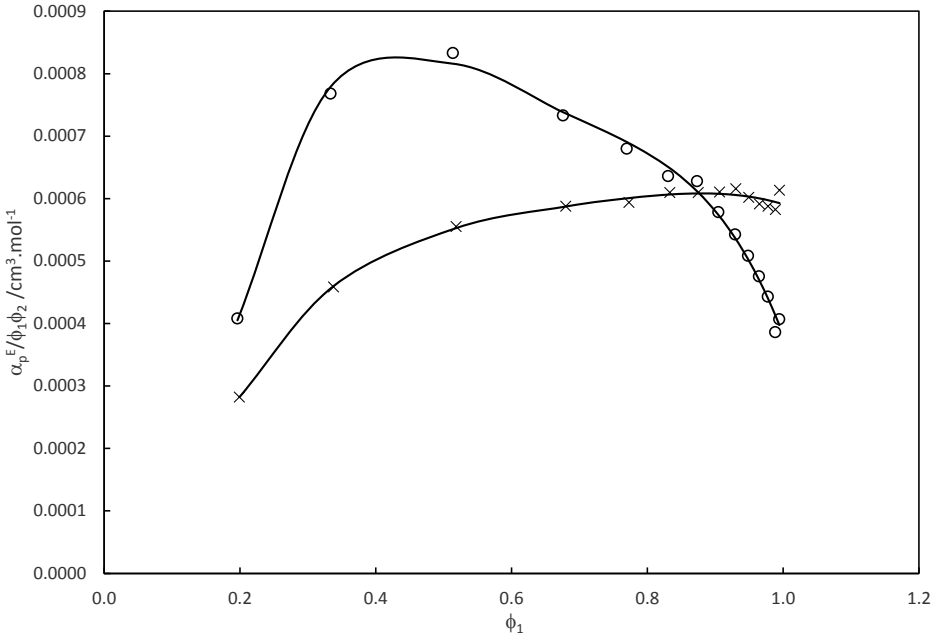

Figure 6: $\frac{\alpha_p{}^E}{\phi_1\phi_2}$ for DEAE-EO (1) + water (2) system as a function of DEAE-EO mole fraction at atmospheric pressure and 2 different temperatures: (○) 293.15 K, (×) 328.15 K, solid line: Redlich-Kister correlation.

3.5. Viscosity

As mentioned above, the kinematic viscosity data are considered. The results are presented in Table 7. Values of kinematic viscosities are presented in Supporting information (Table S5). Globally, the kinematic viscosities increase with increasing DEAE-EO concentration and reach a maximum at composition close to 0.3-0.4 and then decrease. Using eqs. 18 to 21, we have considered excess Gibbs free energy of flow and correlated it using the Redlich-Kister equation. Also, we have considered Redlich Kister treatment with 5 parameters. The Redlich-Kister parameters for the determination of excess activation Gibbs free energy are presented in Table 8. Figure 7 shows the excess Gibbs free energy of flow for DEAE-EO (1) + water (2) binary system over the whole range of compositions and at 293.15 and 318.15 K. Also, we can observe an increase of the excess Gibbs free energy of flow with increasing concentration. The maximum is reached at a concentration close to 0.3. We can also observe that an increasing temperature decreases the excess Gibbs free energy of flow and so reduces kinematic viscosity. The concentration of the maximum remains constant. The reason of this maximum can be attributed to the appearance of a complex with strong molecular interaction between water and DEAE molecules. The composition of the maximum corresponds to the composition that corresponds to the maximum of excess squared refractive index (Fig. S4) but not the minimum of excess volume (Fig. 3). According the Eyring theory, the excess Gibbs free energy of flow is linked to the excess Gibbs free energy calculated with the activity coefficient. At the composition of the maximum, strong molecular interaction certainly exists and, consequently, difficulty to flow might appear. So, more energy is required to move the molecules by breaking the molecular interaction. This phenomenon was already modelled by Grunberg and Nissan [21], and further discussed by Fort and Moore [22]. Similar conclusions have been formulated by Wiseman et al. [23] for the binary system 2-(2-butoxyethoxy)ethanol with aniline and N-alkyl anilines and Aswasthi et al. [24] for the binary system formamide + 2-alkoxyethanols. As we have performed the measurement at several temperatures, it is possible to calculate the excess entropy of flow (ΔS^{*E}) considering Eq. 32.

$$\Delta S^{*E} = -\left(\frac{\partial \Delta G^{*E}}{\partial T}\right)_P \tag{32}$$

Using our data, we have plotted in Fig. 8 the excess entropy of flow for the DEAE-EO (1) + water (2) binary system over the whole range of concentrations. The trend is the same as for the excess Gibbs free energy of flow. It confirms that molecular interactions between DEAE-EO and water are very strong, especially at the composition of the maximum. Also, we observe an effect of temperature for compositions from $x_{DEAE\text{-}EO}$=0.5 to 1. Comparing to the excess thermal expansion (Fig. 5), we suspect

the same temperature effect, but that was not observed for the excess molar volume (Fig. 3). It can be a consequence of the fact that the $\frac{{\alpha_p}^E}{\phi_1\phi_2}$ linked to apparent molar thermal expansion is almost constant for compositions of DEAE-EO higher than 0.5. It could be very interesting to realize heat capacity measurements on this system and to check if this phenomenon can also be observed.

Table 7: Dynamic viscosity[*] and excess Gibbs free energy of flow[**] (ΔG^{*E}) for DEAE-EO *(1)* + water *(2)* binary system as a function of DEAE-EO mole fraction at atmospheric pressure (p=101.33 kPa)[a]

x_1	η /mPa.s	ΔG^{*E}_1/kJ.mol^{-}	η /mPa.s	ΔG^{*E}_1/kJ.mol^{-}	η /mPa.s	ΔG^{*E}/kJ.mol^{-1}	η /mPa.s	ΔG^{*E}/kJ.mol^{-1}	η /mPa.s	ΔG^{*E}/kJ.mol^{-1}
	T=283.15 K		T=288.15 K		T=293.15 K		T=298.15 K		T=303.15 K	
0	1.306		1.138		1.002		0.890		0.797	
0.0250	3.622	2.241	2.962	2.136	2.469	2.046	2.087	1.965	1.789	1.894
0.0500	7.652	3.847	5.966	3.664	4.764	3.503	3.880	3.361	3.217	3.236
0.1000	18.262	5.613	13.618	5.365	10.440	5.146	8.179	4.946	6.547	4.769
0.1799	33.240	6.590	24.439	6.342	18.488	6.122	14.073	5.882	10.981	5.670
0.2600	41.358	6.670	30.121	6.417	22.513	6.183	17.210	5.969	13.342	5.755
0.3400	43.622	6.358	31.739	6.113	23.707	5.887	18.147	5.685	13.981	5.463
0.4199	41.157	5.782	30.092	5.554	22.612	5.348	17.403	5.163	13.516	4.966
0.4998	37.381	5.114	27.755	4.926	21.149	4.757	16.909	4.671	13.240	4.499
0.5803	31.824	4.288	23.945	4.133	18.490	3.997	14.348	3.838	11.352	3.691
0.6592	30.117	3.719	20.504	3.329	16.091	3.233	12.680	3.112	10.138	2.993
0.7408	25.208	2.843	17.708	2.529	13.367	2.339	11.072	2.340	8.990	2.260
0.8203	21.032	1.972	15.189	1.723	12.025	1.650	9.708	1.589	7.975	1.539
0.9004	16.767	0.988	13.622	1.020	10.654	0.919	8.687	0.884	7.191	0.854
0.9503	15.239	0.482	12.126	0.465	9.830	0.451	8.069	0.433	6.724	0.421
1	13.984		11.203		9.131		7.546		6.318	

[a]Expanded uncertainties (k=2) U(P)=0.3 kPa, U(*T*)=0.01 K, U(α)=2.2 10^{-5}K^{-1} , U(*x*)=0.002, $U_r(\eta)$=0.01, U(ΔG^E)=0.002 kJ.mol^{-1}

[*]: measured, [**]: calculated

Table 7: Continued

x_1	η /mPa.s	ΔG^{*E}_1/kJ.mol^{-1}	η /mPa.s	ΔG^{*E}_1/kJ.mol^{-1}	η /mPa.s	ΔG^{*E}/kJ.mol^{-1}	η /mPa.s	ΔG^{*E}/kJ.mol^{-1}	η /mPa.s	ΔG^{*E}/kJ.mol^{-1}
	T=308.15 K		T= 313.15 K		T=318.15 K		T=323.15 K		T=328.15 K	
0	0.719		0.653		0.596		0.547		0.504	
0.0250	1.553	1.833	1.357	1.768	1.200	1.718	1.070	1.673	0.962	1.637
0.0500	2.709	3.125	2.313	3.026	1.998	2.940	1.744	2.862	1.538	2.797
0.1000	5.333	4.608	4.413	4.461	3.703	4.330	3.145	4.208	2.700	4.099
0.1799	8.745	5.479	7.070	5.298	5.802	5.133	4.826	4.981	4.064	4.841
0.2600	10.516	5.552	8.458	5.371	6.886	5.198	5.684	5.036	4.752	4.889
0.3400	11.016	5.267	8.845	5.089	7.195	4.921	5.931	4.762	4.952	4.617
0.4199	10.686	4.783	8.618	4.621	7.035	4.465	5.819	4.320	4.871	4.186
0.4998	10.719	4.381	8.622	4.218	7.060	4.075	5.889	3.958	4.944	3.836
0.5803	9.135	3.557	7.471	3.435	6.183	3.320	5.181	3.213	4.390	3.116
0.6592	8.248	2.887	6.807	2.790	5.679	2.697	4.793	2.611	4.089	2.532
0.7408	7.395	2.183	6.156	2.110	5.184	2.041	4.413	1.979	3.790	1.920
0.8203	6.625	1.488	5.569	1.440	4.730	1.395	4.056	1.353	3.508	1.313
0.9004	6.028	0.827	5.104	0.800	4.368	0.776	3.770	0.753	3.278	0.728
0.9503	5.667	0.408	4.825	0.395	4.148	0.384	3.596	0.374	3.142	0.363
1	5.349		4.575		3.949		3.436		3.013	

[a]Expanded uncertainties (k=2) U(P)=0.3 kPa, U(T)=0.01 K, U(α)=2.2 10^{-5}K^{-1} , U(x)=0.002, $U_r(\eta)$=0.01., U(ΔG^E)=0.002 kJ.mol^{-1}

Table 7: Continued

x_1	η /mPa.s	ΔG^{*E}/kJ.mol^{-1}	η /mPa.s	ΔG^{*E}/kJ.mol^{-1}	η /mPa.s	ΔG^{*E}/kJ.mol^{-1}
	T=333.15 K		T=338.15 K		T=343.15 K	
0	0.466		0.433		0.404	
0.0250	0.870	1.605	0.791	1.573	0.724	1.546
0.0500	1.363	2.731	1.219	2.674	1.099	2.625
0.1000	2.343	4.002	2.051	3.911	1.810	3.827
0.1799	3.456	4.711	2.971	4.590	2.577	4.477
0.2600	4.018	4.753	3.420	4.615	2.946	4.492
0.3400	4.180	4.483	3.567	4.357	3.073	4.240
0.4199	4.123	4.062	3.524	3.944	3.040	3.834
0.4998	4.194	3.722	3.598	3.619	3.113	3.522
0.5803	3.754	3.023	3.240	2.936	2.820	2.855
0.6592	3.521	2.459	3.054	2.387	2.673	2.324
0.7408	3.283	1.864	2.866	1.811	2.522	1.764
0.8203	3.058	1.276	2.685	1.239	2.373	1.205
0.9004	2.876	0.709	2.537	0.687	2.254	0.669
0.9503	2.765	0.353	2.450	0.344	2.183	0.335
1	2.661		2.365		2.113	

[a]Expanded uncertainties (k=2) U(P)=0.3 kPa, U(T)=0.01 K, U(α)=2.2 10^{-5}K^{-1} , U(x)=0.002, U$_r$(η)=0.01., U(ΔG^E)=0.002 kJ.mol^{-1}

Table 8: Excess Gibbs energy of flow: Redlich-Kister parameters and deviation for DEAE-EO + water binary system.

T/K	Redlich Kister parameters										Variance σ/ kJ.mol^{-1}, eq.20
	A_0	u(A_0)	A_1	u(A_1)	A_2	u(A_2)	A_3	u(A_3)	A_4	u(A_4)	
283.15	8.727	0.009	-6.318	0.029	5.44	0.09	-11.41	0.07	8.91	0.15	0.061
288.15	8.239	0.006	-6.704	0.020	3.66	0.06	-9.53	0.05	10.55	0.10	0.038
293.15	7.823	0.003	-6.417	0.009	3.20	0.03	-9.02	0.02	10.05	0.05	0.031
298.15	7.456	0.003	-6.043	0.010	3.04	0.03	-8.51	0.02	9.32	0.05	0.032
303.15	7.052	0.003	-5.713	0.009	2.97	0.03	-8.07	0.02	8.77	0.04	0.031
308.15	6.708	0.003	-5.410	0.009	2.70	0.03	-7.70	0.02	8.52	0.04	0.030
313.15	6.368	0.002	-5.146	0.007	2.66	0.02	-7.34	0.02	8.02	0.04	0.028
318.15	6.056	0.002	-4.889	0.007	2.56	0.02	-7.05	0.02	7.70	0.03	0.027
323.15	5.777	0.002	-4.644	0.007	2.41	0.02	-6.81	0.02	7.48	0.03	0.027
328.15	5.514	0.002	-4.415	0.006	2.30	0.02	-6.62	0.02	7.26	0.03	0.026
333.15	5.271	0.002	-4.208	0.006	2.20	0.02	-6.43	0.01	7.06	0.03	0.025
338.15	5.047	0.002	-4.009	0.006	2.06	0.02	-6.27	0.01	6.94	0.03	0.025
343.15	4.839	0.002	-3.821	0.005	1.94	0.02	-6.13	0.01	6.81	0.03	0.024

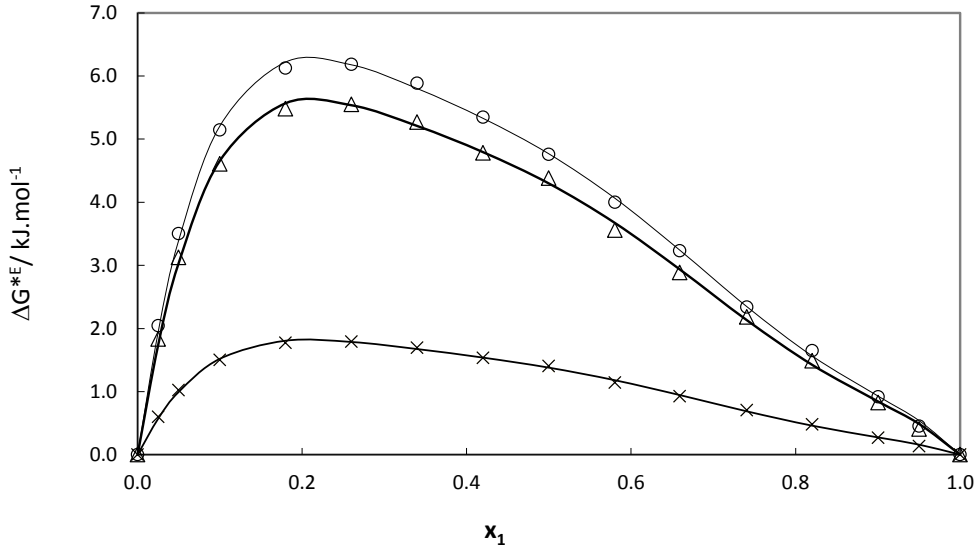

Figure 7: Excess Gibbs free energy of flow for DEAE-EO (1) + water (2) binary system as a function of DEAE-EO mole fraction at atmospheric pressure and for 3 different temperatures. (○) 293.15 K, (Δ) 308.15 K, (×) 328.15 K, solid line: Redlich-Kister correlation.

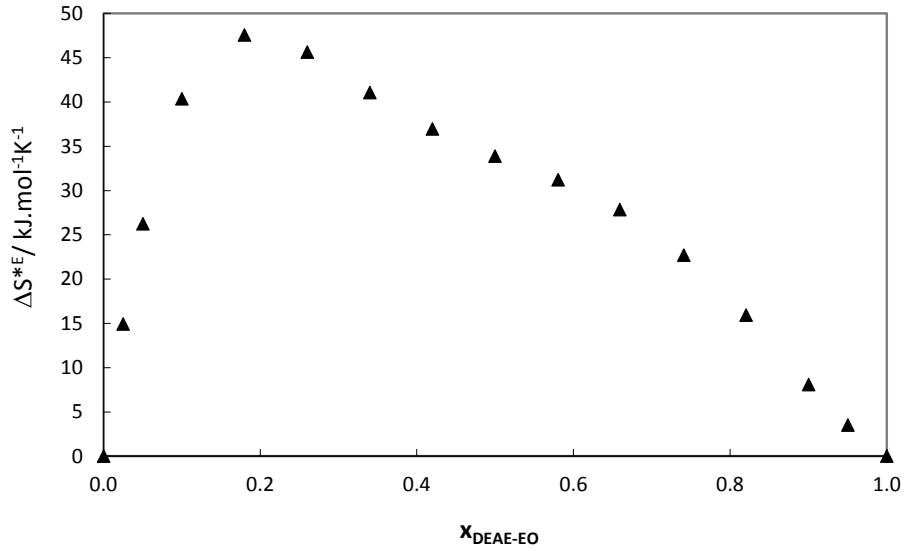

Figure 8: Excess entropy of flow for DEAE-EO (1) + water (2) binary system for the whole range of mole fractions.

4. Discussion

Using the same equipment, we have measured the density and dynamic viscosity of an aqueous DEAE-EO mixture (13 mol%) and compared to the benchmark solvent used in gas processing: aqueous MDEA(13 mol%). Table 9 presents our results.

Table 9: Density and dynamic viscosity values for the aqueous DEAE-EO and MDEA 13 mol% solvents at atmospheric pressure (p=101.33 kPa)[a].

	DEAE-EO (x=0.1304)		MDEA (x=0.1299)	
T/K	ρ /kg/m^3	η /mPa.s	ρ /kg/m^3	η /mPa.s
283.15	1009	25.392	1053	19.360
285.15	1007	22.490	1052	17.510
287.15	1006	20.094	1051	15.730
289.15	1004	18.044	1049	14.190
291.15	1003	16.055	1048	12.830
293.15	1001	14.312	1047	11.650
295.15	1000	12.770	1046	10.590
297.15	998	11.465	1045	9.678
299.15	996	10.310	1043	8.811
301.15	995	9.342	1042	8.090
303.15	993	8.471	1041	7.436
305.15	991	7.716	1040	6.856
307.15	990	7.055	1038	6.331
309.15	988	6.491	1037	5.866
311.15	986	5.984	1036	5.433
313.15	985	5.545	1034	5.058
315.16	983	5.130	1033	4.710
317.15	981	4.777	1032	4.395
319.15	980	4.435	1030	4.113
321.15	978	4.145	1029	3.850
323.15	976	3.875	1027	3.615
325.15	975	3.629	1026	3.397
327.15	973	3.403	1025	3.200
329.15	971	3.195	1023	3.013
331.15	969	3.007	1022	2.847
333.15	968	2.837	1020	2.686
335.15	966	2.670	1019	2.546
337.15	964	2.532	1017	2.410
339.15	962	2.394	1016	2.287
341.15	961	2.269	1014	2.172
343.15	959	2.152	1013	2.066

[a]Expanded uncertainties (k=2) U(p)=0.3 kPa, U(T)=0.01 K, U(ρ)=1.0 kg.m^{-3} U(x)=0.002, U$_r$(η)=0.01.

To correlate our results, we have considered for the densities a second order polynomial expression (Eq. 33) and an Arrhenius type law (Eq. 34).

$$\rho = AT^2 + BT + C \quad (33)$$

$$ln(\eta) = A + \frac{B}{T} \quad (34)$$

To estimate the diffusion coefficient of CO_2 in the solvent, we have considered the Stokes-Einstein relation where $D_A \mu_L^p = Constant$. Versteeg et al. [25] have applied this relation by considering p=0.8 (Eq. 35). For the diffusion coefficient of CO_2 into pure water and for the viscosity of pure water we have used the correlations presented in the Versteeg et al. paper.

$$D_{CO2}^{Solvent} = D_{CO2}^{eau} \left(\frac{\mu_{H2O}}{\mu_{Solvent}}\right)^{0.8} \quad (35)$$

An Arrhenius type law is also considered to correlate the predicted diffusion coefficient of CO_2 (Eq. 36).

$$ln\left(D_{CO_2}\right) = A + \frac{B}{T} \quad (36)$$

Table 10 presents the parameters for the 3 different equations and their corresponding standard deviations.

The Schmidt number is calculated using the thermophysical properties. As an example, we have calculated the Schmidt number for CO_2. (Eq. 37).

$$Sc = \frac{\eta}{\rho D_{CO_2}} \quad (37)$$

The Schmidt number depends on thermophysical properties. It is the ratio between the viscous diffusion rate and the molecular diffusion rate. The smaller the Sc, the more preponderant the diffusion is.

For example, at 323.15 K, the value for the Schmidt number is equal to 6021 and 5011 for 13 mol% DEAE-EO and 13 mol% MDEA aqueous solvents, respectively. It signifies that independently of the conditions of chemical reaction between the solvent and the CO_2, the flux of absorption will be faster with MDEA 13 mol% aqueous solvent. It is an important information to consider in the estimation of mass transfer coefficient in the context of acid gas absorption or CO_2 capture by chemical solvent.

Additional results concerning speed of sound and refractive index (for each pure component and mixtures) and are presented in the Supporting Information.

Table 10: Correlations parameters for the calculation of density, dynamic viscosity and CO_2 diffusion coefficient.

	A	u(A)	B	U(B)	C	U(C)
DEAE-EO 13 mol%						
Density / kg/m^3	-0.0001039	6.9 10^{-6}	-0.1851	0.004	1144.67	0.7
Dynamic viscosity/ mPa.s	-17.83	0.19	3976	58	-	-
CO_2 diffusion coefficient /m^2s^{-1}	-9.62	0.15	-3722	46	-	-
MDEA 13 mol%						
Density / kg/m^3	-0.00164	0.8 10^{-5}	0.3548	0.0051	1083.78	0.81
Dynamic viscosity/ mPa.s	-16.76	0.12	3607	39	-	-
CO_2 diffusion coefficient /m^2s^{-1}	-10.47	0.10	-3426	31	-	-

5. Conclusion

The densities, viscosities, speed of sound and refractive index of the DEAE-EO + water binary system were measured over the temperature range T=[283.15 – 343.15 K] using various instruments (vibrating tube densitometer, falling ball viscometer and refractometer). Excess molar volume, thermal expansion and excess Gibbs free energy of flow were determined and correlated by a Redlich-Kister correlation. The addition of DEAE-EO to water increases the density with a maximum around 10 mol%, indicating a stronger packing, probably due to the hydrophobic effect and intermolecular hydrogen bonding. The two hydrophobic ethyl groups of DEAE-EO result in clustering of DEAE-EO and force the water to break its hydrogen-bond structure and to reorganize around the hydrophobic parts. Water can also form hydrogen bonds with the ethoxy and alkanol group of DEAE-EO, resulting in denser packing. In line with this, aqueous DEAE-EO shows a strongly negative excess volume (minimum around 30-40 mol%). The excess volume of aqueous DEAE-EO, expressed as v^E/x_1x_2 is very similar to aqueous DEAE (the ethoxy group seems to have little impact), but shows a much lower negative value at infinite dilution than aqueous MDEA. This is likely the result of the hydrophobic effect (DEAE-EO and DEAE have only one -OH group, while MDEA has two). Due to this

hydrophobic effect DEAE-EO is a (water) structure maker. This is confirmed by the positive sign of $\left(\frac{\partial C_P}{\partial P}\right)_T$. The excess Gibbs free energy of flow shows a maximum around 30 mol% DEAE-EO. The strong excess intermolecular interactions will impact the CO_2 absorption properties.

Supporting information Available:

It presents comparison with literature data, the correlation used to calculate the molar volumes, the results concerning the speed of sound measurements, kinematic viscosities, refractive index and the method used to calculate the standard deviation of the Redlich-Kister parameters correlation.

References

[1] Chowdhury, F. A.; Okabe, H.; Shimizu, S.; Onoda, M.; Fujioka, Y. Development of novel tertiary amine absorbents for CO2 capture, Energy Procedia 1 (2009) 1241-1248. https://doi.org/10.1016/j.egypro.2009.01.163

[2] Chowdhury, F. A.; Higashii, T.; Goto, K.; Onoda, M.; Kazama, S. Synthesis and selection of new amine absorbents for CO2 capture 1st Post Combustion Capture Conference 2011. Presentation available online: https://ieaghg.org/docs/General_Docs/PCCC1/Presentations/4_PCCCI_Session%201a_Firoz%20A.%20Chowdhury.pdf

[3] Hartono, A.; Vevelstad, S. J.; Ciftja, A.; Knuutila, H.K. Screening of strong bicarbonate forming solvents for CO2 capture Int. J. of Greenh. Gas Control 58 (2017) 201-211. https://doi.org/10.1016/j.ijggc.2016.12.018

[4] Shoukat, U.; Pinto, D.D.D.; Knuutila, H.K. Study of Various Aqueous and Non-Aqueous Amine Blends for Hydrogen Sulfide Removal from Natural Gas. Processes 7 (2019) 160 https://doi.org/10.3390/pr7030160

[5] Orlov, A.A.; Demenko, D.Y.; Bignaud, C.; Valtz, A.; Marcou, G.; Horvath, D.; Coquelet, C.; Varnek, A.; de Meyer, F. Chemoinformatics-Driven Design of New Physical Solvents for Selective CO2 Absorption. Environ. Sci. & Technol. 55 (2021) 15542-15553. https://doi.org/10.1021/acs.est.1c04092

[6] Orlov, A.A.; Valtz, A. ; Coquelet, C. ; Rozanska, X. ; Wimmer, E. ; Marcou, G. ; Horvath, D. ; Poulain, B.; Varnek, A.; de Meyer, F. Computational screening methodology identifies effective solvents for CO2 capture. Commun. Chem. 5 (2022)37 https://doi.org/10.1038/s42004-022-00654-y

[7] Malwitz, N.; Wong, S.W.; Frisch, K.C.; Manis, P.A. Amine catalysis of polyurethane foams. Journal of cellular plastics 23 (1987) 461-502. https://doi.org/10.1177/0021955X8702300505

[8] Datasheet from TCI https://images-na.ssl-images-amazon.com/images/I/4191TZv75fL.pdf (accessed 17 April 2023)

[9] Pubchem Web site: https://pubchem.ncbi.nlm.nih.gov/compound/2-Diethylaminoethanol (accessed 13 April 2023).

[12] Redlich, O.; Kister, A. Algebraic Representation of Thermodynamic Properties and the Classification of Solutions Ind. Eng. Chem. 1948, 40, 345–348. https://doi.org/10.1021/ie50458a036

[11] Chirico, R. D.; Frenkel, M.; Magee, J. W.; Diky, V.; Muzny, C. D.; Kazakov, A. F.; ... & Wu, J. Improvement of quality in publication of experimental thermophysical property data: Challenges, assessment tools, global implementation, and online support. J. Chem. Eng. Data 58 (2013) 2699-2716. https://doi.org/10.1021/je400569s

[12] Reference Manual Lovis 2000 M/ME, Instrument Software version : 2.30-Build 245 and Instrument Software version : 2.32-Build 32, Anton Paar GmbH, Graz, Austria, November 2012

[13] Cremona, R.; Delgado, S.; Valtz, A.; Conversano, A.; Gatti, M.; Coquelet, C. Density and Viscosity Measurements and Modeling of CO2-Loaded and Unloaded Aqueous Solutions of Potassium Lysinate J. Chem. Eng. Data 66 (2021) 4460-4475. https://doi.org/10.1021/acs.jced.1c00520

[14] Huber, M. L.; Perkins, R. A.; Laesecke, A.; Friend, D. G.; Sengers, J. V. New international formulation for the viscosity of H2O J. Phys. Chem. Ref. Data 38 (2009) 101-125. https://doi.org/10.1063/1.3088050

[15] Eyring, H. Viscosity, plasticity, and diffusion as examples of absolute reaction rates J. Chem. Phys. 4 (1936) 283-291. https://doi.org/10.1063/1.1749836

[16] Desnoyers, J.; Perron, G. Treatment of Excess Thermodynamic Quantities for Liquid Mixtures J. Solution Chem. 26 (1997) 749–755. https://doi.org/10.1007/BF02767781

[17] Hepler, L.G. Thermal expansion and structure in water and aqueous solutions Can. J. Chem. 47 (1969) 4613-4617. https://doi.org/10.1139/v69-762

[18] Coquelet, C., Awan, J. A., Valtz, A., Richon, D. Volumetric properties of hexamethyleneimine and of its mixtures with water. Thermochimica acta 484 (2009) 57-64. https://doi.org/10.1016/j.tca.2008.12.007

[19] Bernal-García, J. M., Ramos-Estrada, M., Iglesias-Silva, G. A., Hall, K. R. Densities and excess molar volumes of aqueous solutions of n-methyldiethanolamine (MDEA) at temperatures from (283.15 to 363.15) K. J. Chem. Eng. Data 48(2003) 1442-1445. https://doi.org/10.1021/je030120x

[20] Ma, D., Zhu, C., Fu, T., Yuan, X.,Ma, Y. Volumetric and viscometric properties of binary and ternary mixtures of monoethanolamine, 2-(diethylamino) ethanol and water from (293.15 to 333.15) K. J. Chem. Therm. 138 (2019) 350-365 https://doi.org/10.1016/j.jct.2019.06.032

[21] Grunberg, L., Nissan, A. Mixture Law for Viscosity. Nature 164 (1949) 799–800. https://doi.org/10.1038/164799b0

[22] Fort, R. J., Moore, W.R. Viscosities of binary liquid mixtures. Trans. Faraday Soc. 62 (1966) 1112-1119 https://doi.org/10.1039/TF9666201112

[23] Wiseman, P., Heggie, M., Palepu, R. Viscosities and thermodynamics of viscous Flow of binary liquid mixtures of 2-(2-butoxyethoxy)etanol with aniline nd N-alkyl anilines. Can. J. Chem. 70 (1992) 2645-2649. https://doi.org/10.1139/v92-333

[24] Awasthi, A., Awasthi, A. Intermolecular interactions in formamide + 2-alkoxyethanols: Viscometric study. Thermochim. Acta 537(2012) 57-64. https://doi.org/10.1016/j.tca.2012.03.001

[25] Versteeg, G.F., van Swaalj, W.P.M. Solubility and diffusivity of acid gases (CO2, N2O) in aqueous alkanolamines solutions, J. Chem. Eng. Data 33(1988) 29-34. https://doi.org/10.1021/je00051a011

GRAPHICAL ABSTRACT